J Nanostruct 13(1): 132-145, Winter 2023

RESEARCH PAPER

Analysis of the Effect of TDS on the Stability of Nanoemulsified Oil

Wei Zhang

School of Chemical Engineering and Technology, Sun Yat sen University, Guangzhou, China

ARTICLE INFO

Article History:
Received 11 October 2022
Accepted 23 December 2022
Published 01 January 2023

Keywords:
Brownian motion
Groundwater
Nanoemulsified oil
Stability
TDS

ABSTRACT

In this paper, we designed a batch experimental protocol for the effect of groundwater TDS on the stability of prepared nanoemulsified oils by artificially simulating the preparation of natural groundwater and characterizing the dynamic changes of nanoemulsified oil particle size, backscattered light flux, photon free range, and peak thickness under the influence of TDS using dynamic light dispersion and multiple light dispersion techniques, respectively. The stability of nanoemulsified oil was positively affected by TDS at 400, 600 and 1000 mg/L. The TSI increased and then decreased with the increase of TDS, and the stability of nanoemulsified oil increased by 63.70 %, 57.53 % and 15.07 % compared to the blank sample, respectively. The instability of the top instability zone of nanoemulsified oil was mainly influenced by droplet floating and aggregation, while the decrease of the volume fraction of nanoemulsified oil in the bottom instability zone caused by the influence of floating was the main reason for its instability. Compared with the blank sample, the experimental design of TDS inhibited the floating phenomenon of nanoemulsified oil and the aggregation of droplets, and gradually weakened with increasing concentration. 400 mg/L sample reduced the two instability factors by 87.5% and 87.2%, respectively. Therefore, the appropriate groundwater TDS can weaken the Brownian motion and reduce the upwelling and aggregation phenomena, which can positively affect the stability of nanoemulsified oil and facilitate the migration of nanoemulsified oil in porous media.

How to cite this article
Zhang W. Analysis of the Effect of TDS on the Stability of Nanoemulsified Oil. J Nanostruct, 2023; 13(1):132-145. DOI: 10.22052/JNS.2023.01.015

INTRODUCTION

Emulsified oil is an emulsion prepared by mixing vegetable oil, edible surfactant, and deionized water in certain proportions, and then by phase ascending temperature transformation technique [1-3]. In the in situ remediation of contaminated groundwater, emulsified oil is used as a long-lasting slow-release carbon source and electron donor [4-5], which is injected in situ into the aquifer to enhance indigenous microorganisms to achieve efficient degradation of contaminants [6-7], such as chloro-scrip, Cr(VI), radioactive U(VI), nitrate, and other contaminants [8-9]. Due to its high kinetic stability [10-11], nanoemulsified oil can form certain reaction zones in the gas envelope and aquifer to achieve in situ remediation of contaminants [12-14]. However, the type of water chemistry, salinity and pH in natural aqueous porous media may affect the surface properties of nanoemulsified oils, further affecting the

* *Corresponding Author Email: liu461461@126.com*

dispersion, migration and release of nanodroplets and hindering the remediation of groundwater contamination [15-16].

Nanoemulsions are a widely used in many fields such as chemicals, food, petroleum, cosmetics, pharmaceuticals and catalysis [17-18]. They have a particle size range of 50 ~ 500 nm, are transparent, translucent or milky white, have moderate emulsifier concentrations, and are characterized by small droplet size, uniform particle size, and long-term kinetic stability [19-21]. To address the problem of reduced remediation efficiency caused by emulsified oil clogging aquifers, if the technical means of preparing nanoemulsions is used to optimize the preparation of emulsified oil into nanoemulsified oil with smaller particle size and inject it into the ground instead of emulsified oil for in situ bioremediation of groundwater pollution, the problem of aquifer permeability loss and clogging caused by emulsified oil can be effectively alleviated [22-24]. Therefore, carrying out the preparation of nanoemulsified oil and studying its retention and release characteristics, permeability loss mitigation, and effective lifetime in the in situ remediation of groundwater contamination is of great practical importance to expand the application of emulsified oil in aquifers [25-26].

Relevant studies in the fields of food and medicine have confirmed that the stability of nanoemulsions is influenced by the ionic strength. In the literature [27-29], it was demonstrated that the average droplet size of nanoemulsified oils prepared with polyoxypropylene surfactants decreased in the system of sodium chloride from 0 to 50 mmol/L, the particle size distribution curve became narrower, the peak became steeper, the surface tension decreased, and it contributed to the destabilization of the emulsion. In the literature [30-31], when simulating the removal of nitrate contamination from groundwater by emulsified oil reaction zone through sandbox experiments, it was found that the permeability loss of porous media was about 27% due to microbial colonization and N2 and CO2 generation. The literature [32-33] confirmed that the addition of different types and concentrations of ions to paraffinic nanoemulsified oils caused changes in the surface zeta potential of droplets and even the inversion of surface charge, and that the effect of higher valence ions on the stability of emulsions was more significant.

Studies in the literature [34-35] showed that emulsified oil injection activated microbial activity in aquifers in site remediation experiments of tetrachloroethylene and chlorinated solvent-contaminated groundwater, and microbial overgrowth led to aquifer permeability losses of up to 39% ~91%. Literature [36-37] demonstrated that β-carotene-rich nanoemulsified oils are prone to droplet aggregation at low pH and high ionic strength due to electrostatic shielding effect. In the literature [38-39], emulsified oil was used as a carbon source to simulate the effect of in situ nitrate remediation through chamber column experiments, and finally it was concluded that the addition of emulsified oil had a good removal effect for nitrate contaminated solutions with feed water concentrations of both 20 mg/L and 50 mg/L, with a maximum removal rate of 99%.

Literature [40-41] pointed out that the adsorption residue of emulsified oil in porous media and the physical retention generated by the particle size of emulsified oil larger than the pore size of aquifer media may also be one of the important reasons for the permeability loss. The results of literature [42-44] show that after emulsified oil is placed into injection wells, its removal effect on pollutants can be maintained for up to 3-5 years because emulsified oil can migrate in a wide range with groundwater flow in underground aquifers, and the effect of fewer injection points and larger migration range can be achieved, thus realizing the purpose of achieving better removal effect with smaller investment cost. In the literature [45-46], when using column experiments to simulate the degradation of nitrobenzene by emulsified oil, it was found that the permeability of the experimental column decreased about 31.5%-72.0% after emulsified oil injection, and the analysis suggested that the accumulation of microbial colonization and emulsified oil sequestration might be the cause of the loss of permeability. In the literature [47-48], the effect of nanoemulsified oil as a carbon source to degrade nitrate nitrogen and the change of microbial population were analyzed by using nanoemulsified oil to enhance the denitrification process of NO3-N. It was shown that 2 ml of nanoemulsified oil could achieve the degradation of nitrate at a concentration of 50 mg/L in 10 denitrification processes with a removal rate of 99.5%.

The above studies have analyzed

nanoemulsified oils from different perspectives, but a comprehensive quantitative analysis of the stability of prepared nanoemulsified oils is lacking. In this paper, the study of the effect of TDS on the stability of prepared nanoemulsified oils was carried out by artificially simulating the preparation of natural groundwater, and the stability of nanoemulsions was comprehensively evaluated based on the study of the changes of nanoemulsified oil particle size, sample local stability, peak thickness and other indicators under the influence of TDS. In particular, the dynamic light dispersion method was used for the determination of nanoemulsified oil particle size, while the overall stability indexes TSI at the top, middle and bottom were determined with the help of multiple light dispersion techniques. Also, the relationship between the variation of the peak thickness in the instability region and the kinetic variation of the stability parameters was analyzed with the help of the variation of the backscattered light intensity in different regions of the sample. In addition, the variation of Brownian motion rate of droplets in nanoemulsified oil with different TDS was also investigated to determine the TDS with the best effect on upwelling phenomenon and aggregation inhibition.

MATERIALS AND METHODS

Materials and Reagents

The nanoemulsified oil preparation materials include: commercially available soybean oil, food grade emulsifiers (tween-80 and Span 80) and deionized water. Among them, tween-80 and Span 80 are nonionic surfactants with hydrophilic and lipophilic balance values of 10 and 4.3, respectively. artificially simulated formulated natural groundwater reagent is $NaHCO_3$, $CaCl_2$, $MgSO_4$.

According to the latest groundwater quality standard GB/T 14848-2017, combined with some actual site testing of in situ groundwater remediation using emulsified oil, the TDS of groundwater is mainly within the range of Class 3 water. The TDS limits of groundwater Class I, Class II and Class III water were selected as the set concentration range, and natural groundwater with different TDS was prepared by manual simulation using stratigraphic simulated water preparation and TDS calculation program. 0.325 g of calcium chloride, 0.175 g of magnesium sulfate and 0.44 g of sodium bicarbonate were added into 1 L of deionized water, and groundwater with TDS of 1000 mg/L was obtained after full dissolution. The measured result was 998.12 mg/L, with a negligible error of 0.19%. The water chemistry was HCO_3-Cl-Ca-Na type, and the main ionic components were shown in Table 1. The ionic fraction content of the groundwater with TDS of 1000 mg/L was calculated by the formulation, while the ionic fraction content of the groundwater with 400 mg/L and 600 mg/L was calculated based on the Phreeqc software, and the errors were below 6.23%.

Experimental protocol design

Based on the method proposed in this paper to prepare nanoemulsified oil, soybean oil, tween-80, Span 80 and prepared groundwater with different TDS were mixed in certain proportions to prepare nanoemulsified oil by ascending phase transfer technique. Table 2 shows the experimental protocol design. A total of four groups of experiments were designed to investigate the effects of simulated groundwater with TDS concentrations of 400, 600 and 1000 mg/L on the properties of nanoemulsified oil using nanoemulsified oil formulated with deionized water as a blank control. Two parallel samples were designed for each group, totaling 8 samples. The properties of nanoemulsified oil such as particle size, zeta potential and stability were determined within 24 hours, and the stability was measured for 5 hours and 40 minutes.

Nano emulsified oil particle size and stability test

A Malvern dynamic light scattering instrument was used to determine the particle size of nanoemulsified oil in the range of 0.3 nm ~ 5 μm, and the temperature was set at 25 °C.

Table 1. The main ionic content of the proposed groundwater (mg/L)

Type of groundwater	Na^+	Ca^{2+}	Mg^{2+}	Cl^-	HCO_3^-	SO_4^{2-}
400 TDS	47	49.1	21.5	84.3	166.1	57.4
600 TDS	70.7	69.3	30.3	125.8	240	85.6
1000 TDS	117.2	118.2	36.4	210.8	310.5	143.8

Table 2. Design of experiments

TDS	Soybean oil/ tween-80/ Span 80 (g)	Water for different TDS (g)	Sample number
Blank	14.5/11/5	75	(1), (2)
400 mg/L			(3), (4)
600 mg/L			(5), (6)
1000 mg/L			(7), (8)

The stability of nanoemulsified oil was tested by multiple light scattering instrument with the accuracy of 0.1 μm ~ 1 mm.The multiple light scattering technique is to measure the sample every 20 μm from the bottom of the cuvette to the top of the cuvette by emitting a near-infrared light source, and completing the measurement from the bottom to the top of the cuvette is called one scan. The variation of the received transmitted and backscattered light is then used to obtain the temporal and spatial variation characteristics of the particle size and concentration of the sample, and thus the stability of the sample. The transmitted and backscattered light intensities are related to the volume concentration and particle size of the sample. If the sample is transparent, the variation of transmitted light intensity is bounded by 2000 nm and shows a trend of decreasing and then increasing. Since the nanoemulsified oil is an opaque emulsion, the intensity of transmitted light is not considered in this experiment. While the intensity of backscattered light increases with the increase of volume concentration, when the particle size is less than 600 nm, the intensity of backscattered light increases with the increase of particle size. When the particle size is larger than 600 nm, the intensity of the backscattered light decreases with the increase of the particle size. After the sample was prepared and its temperature was reduced to room temperature, then the measurement was started and the measurement time was 5 hours and 40 minutes.

Data processing

The multiple light scattering technique can characterize the stability of a disperse system by monitoring the droplet size variation and droplet migration in the disperse system, which has the advantage of obtaining more objective and accurate results without diluting the disperse phase. In multiple light scattering theory, the average photon free range L^* represents the scattering and transmission of light, and its magnitude is related to the droplet size and concentration, which is calculated as:

$$L^* = \frac{2d}{3c(1-g)Q_s} \quad (1)$$

where L^* is the photon free range in μm. d is the droplet diameter in μm. C is the droplet volume ratio, g is the asymmetry factor, and Q_s is the scattering efficiency. Q_s and g are related to the particle size and refractive index, and can be obtained from the Mie light scattering theory.

The backscattered light intensity is related to the concentration and particle size of the sample, specifically the backscattered flux is inversely proportional to the square of the photon free range. The relationship between the backscattered flux and the photon free range is given by the following equation:

$$B = \frac{1}{\sqrt{L^*}} \quad (2)$$

Where B is the backscattered flux and L^* is the photon free range. The photon free range is proportional to the particle size and inversely proportional to the concentration.

The instability kinetic index (TSI) is an evaluation index of the stability of the sample by accumulating the light intensity change values of two scans measured before and after at all heights of the sample, as follows:

$$TSI = \sum_i \frac{\sum_j |B_i - B_{i-1}|}{H} \quad (3)$$

Where i is the i nd measurement, j is the height of the i th measurement, B_i and B_{i-1} are the backscattered fluxes of the i th and i-1 th measurements, respectively. H is the total height

of the sample.

RESULTS AND DISCUSSION

Variation characteristics of average particle size and overall stability of nanoemulsified oil

The variation characteristics of the average particle size and overall stability of nanoemulsified oil under the influence of TDS are shown in Fig. 1. With the increase of TDS, the average particle size and overall stability of nanoemulsified oil showed a trend of decreasing and then increasing in value. Compared with the blank group, the average particle size of nanoemulsified oil decreased by 6.03% and 3.45% under the influence of 400 mg/L and 600 mg/L TDS, respectively. On the contrary, the average particle size of nanoemulsified oil under the influence of 1000 mg/L TDS increased by 6.90%, indicating that the ionic fraction may affect the surface hydration layer and inter-droplet hydrostatic force of the emulsified oil droplets.

For the overall stability index, it reflects the cumulative change of backscattered light intensity over time for the whole system, and the smaller the value, the stronger the stability. From the histogram, it can be seen that although the stability of nanoemulsified oils under the influence of TDS are all at the stability level of A+~B, there are still some differences. Among them, the blank group had the largest TSI index and was relatively less stable. Compared with the blank group, the addition of specific TDS ionic fractions (400, 600 and 1000 mg/L) led to the decrease of the TSI index of nanoemulsified oil by 63.70 %, 57.53 % and 15.07 %, respectively, which effectively improved the stability of nanoemulsified oil. However, with the increase of TDS, the stability enhancement effect of nanoemulsified oil also showed a gradual weakening trend. It can be seen that when the TDS is less than 1000 mg/L, using the solution with suitable TDS concentration to configure nanoemulsified oil can indeed positively affect the properties of nanoemulsified oil, effectively enhance the stability of nanoemulsified oil and improve the application effect of nanoemulsified oil.

In order to further clarify the potential reasons for the influence of TDS on the stability of nanoemulsified oils, the overall variation characteristics of nanoemulsified oils were characterized using backscattered flux (BS). The BS variation of nanoemulsified oil at different TDS is shown in Fig. 2. Based on the variation of the backscattered flux, the nanoemulsified oil samples can be divided into three regions: bottom, middle and top, which are 0 ~ 4 mm, 4 ~ 33.5 mm and 39.5 ~ 42 mm, respectively. among them, the bottom and top of the nanoemulsified oil undergo obvious changes, which show that the BS in the unstable

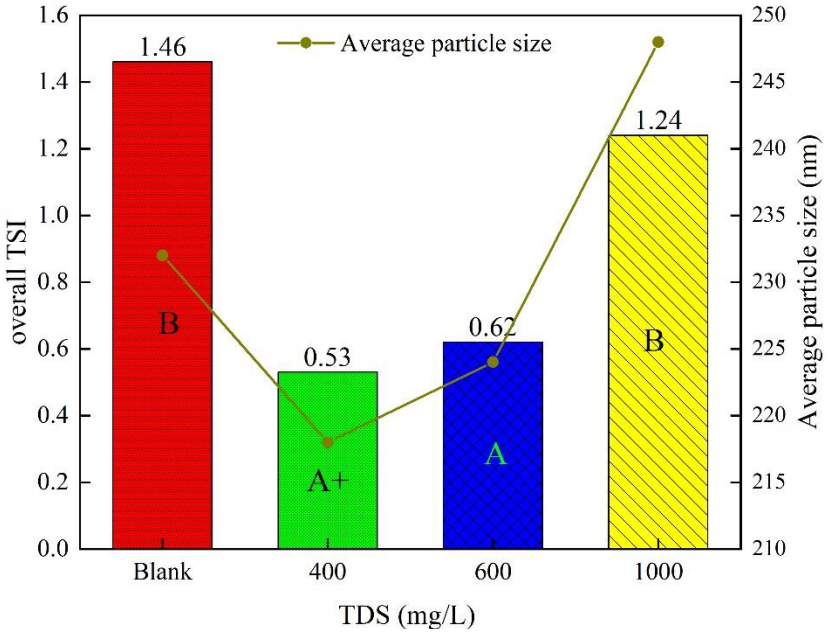

Fig. 1. Average particle size and overall stability under the influence of TDS

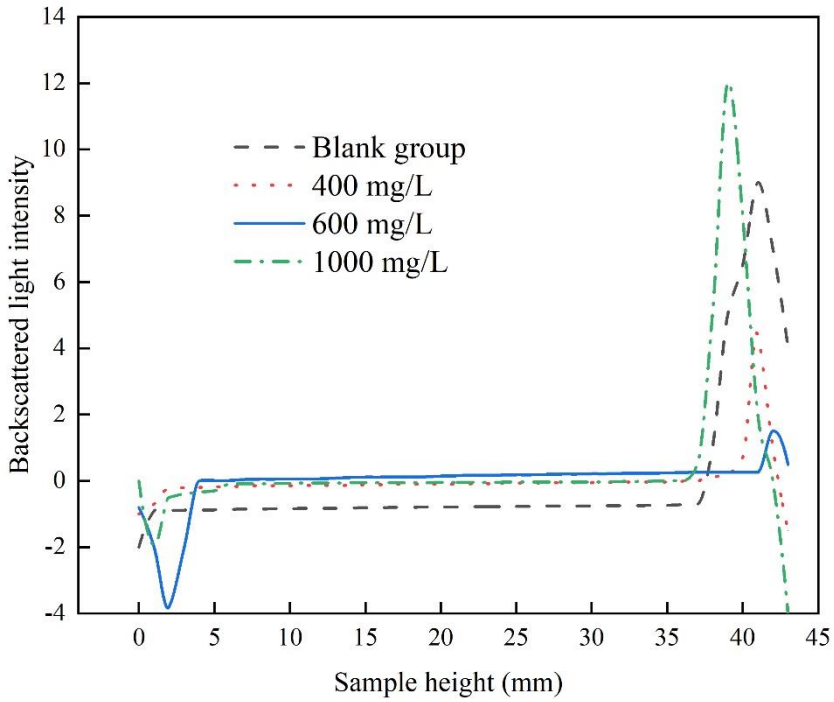

Fig. 2. BS variation of nano-emulsified oil under different TDS

region at the bottom changes more and shows a decreasing trend. The BS in the top unstable zone changes the most and shows an increasing trend. This indicates that the stability of both parts is poor, and there are some differences in the degree of BS decrease and increase under different TDS. There is no significant change in the middle zone, which indicates that the stability of the middle part of the nanoemulsified oil is better under the influence of TDS. Therefore, the next discussion focuses on the effect of TDS on the kinetic changes in the top unstable zone and the bottom unstable zone.

Kinetic variation characteristics of local stability parameters of nanoemulsified oil

Both the overall TSI index and the backscattered light intensity indicate the existence of two instability regions in the nanoemulsified oil samples. The stability of nanoemulsified oil in the local region is directly or indirectly reflected by the local variation characteristics of TSI index, backscattered light intensity, peak thickness and photon free range. The worse the stability of the emulsified oil, the more likely it is to break the emulsion, delamination and other phenomena, which is not conducive to the formation of a stable in-situ restoration reaction zone of the emulsified oil, thus affecting the in-situ restoration treatment effect. Peak thickness is the width of the intersection of the scan peak and the threshold value (the critical backscattered light intensity value of delamination), and its and light intensity change is the specific expression of stability, characterizing the change of delamination thickness and light transmission ability due to particle migration, and to a certain extent can assist in judging the stability of the local area. The larger the peak thickness, the easier the emulsified oil is to agglomerate and delaminate, thus affecting the in-situ remediation treatment. If the peak thickness and light intensity increase gradually with time, it indicates that the more unstable the nanoemulsified oil is, and vice versa, it means that the oil phase in the aqueous phase is less likely to be delaminated and the nanoemulsified oil is more stable.

Kinetic variation of stability parameters in the top instability zone

Fig. 3 shows the kinetic variation characteristics of TSI, peak thickness, BS value and photon free range in the top unstable region of nanoemulsified oil under the influence of TDS. The stability index TSI of the top instability region increased with

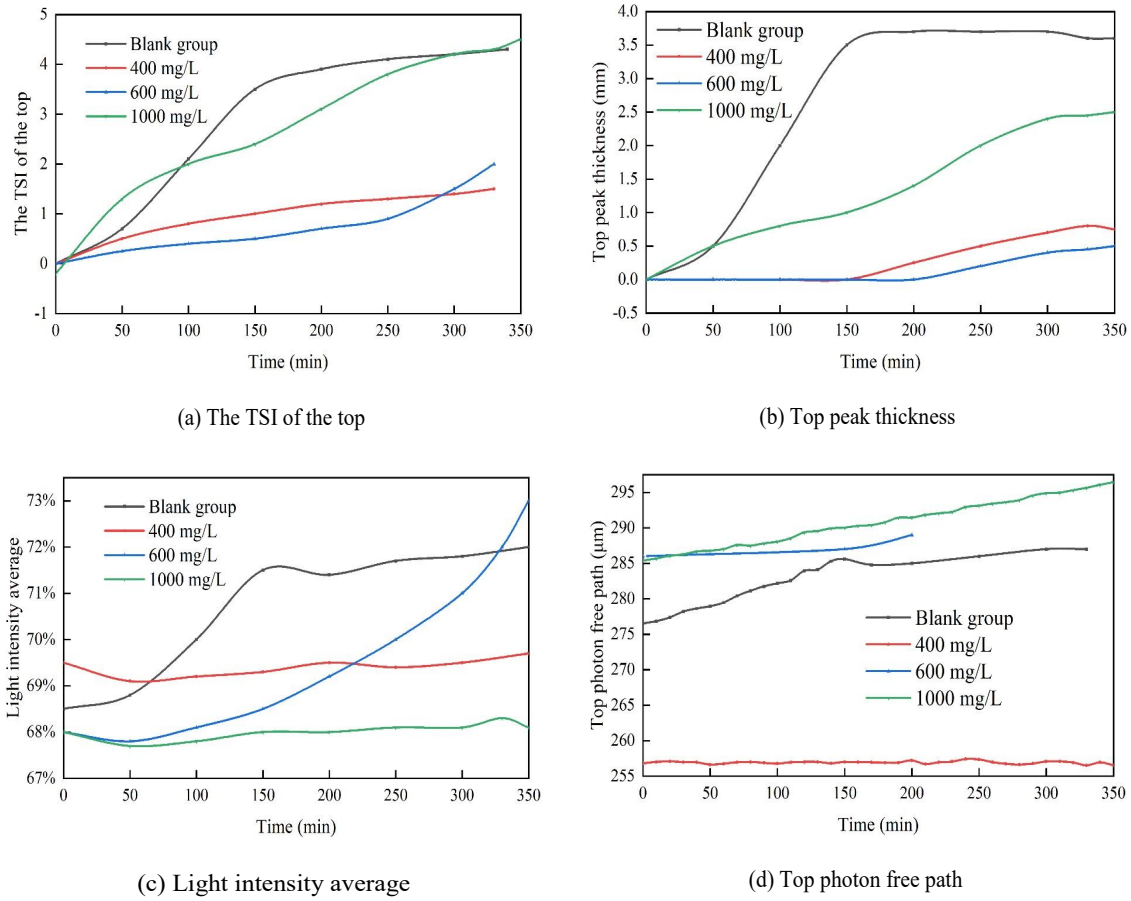

Fig. 3. Changes in indicators at the top under different TDS conditions

time in both the blank group and the specific TDS influence experiments. Among them, the TSI kinetic curves of nanoemulsified oil with TDS concentration of 400 mg/L and 600 mg/L are close, and the variation is only about 1 and the slope of the tangent line is small, which is much lower than the TSI kinetic curves and slope variation of nanoemulsified oil in the blank group and 1000 mg/L. The larger slope indicates that the stability of the nanoemulsified oil in the blank group and 1000 mg/L became less stable in a shorter period of time. It can be seen that a suitable range of TDS (400 ~ 600 mg/L) can effectively enhance the stability of nanoemulsified oil compared with the blank group. However, with the further increase of TDS to 1000 mg/L, this enhancement effect gradually diminished until it disappeared, showing the same results as the blank group.

Fig. 3(b) shows the results of peak thickness variation in the top instability region, and it can be seen that the peak thickness at the top of the nanoemulsified oil in both the blank group and the specific TDS influence experiments showed an increase and then stabilization, i.e., the stratification thickness gradually increased to stability. Among them, the peak thicknesses of the blank group and the samples with 1000 mg/L TDS grew faster, while the nanoemulsified oils with 400 mg/L and 600 mg/L TDS showed a slow growth trend only after 150 and 225 min, respectively, and the top unstable layer did not appear in the early stage. The peak thicknesses of the nanoemulsified oils with TDS concentrations of 400 mg/L and 600 mg/L were the best, followed by the nanoemulsified oils with 1000 mg/L TDS and the worst in the blank group. The degree of light intensity variation from large to small in Fig. 3(c) also shows the same order as the peak thickness, and the visible light intensity variation further illustrates that the TDS of 400 mg/L and

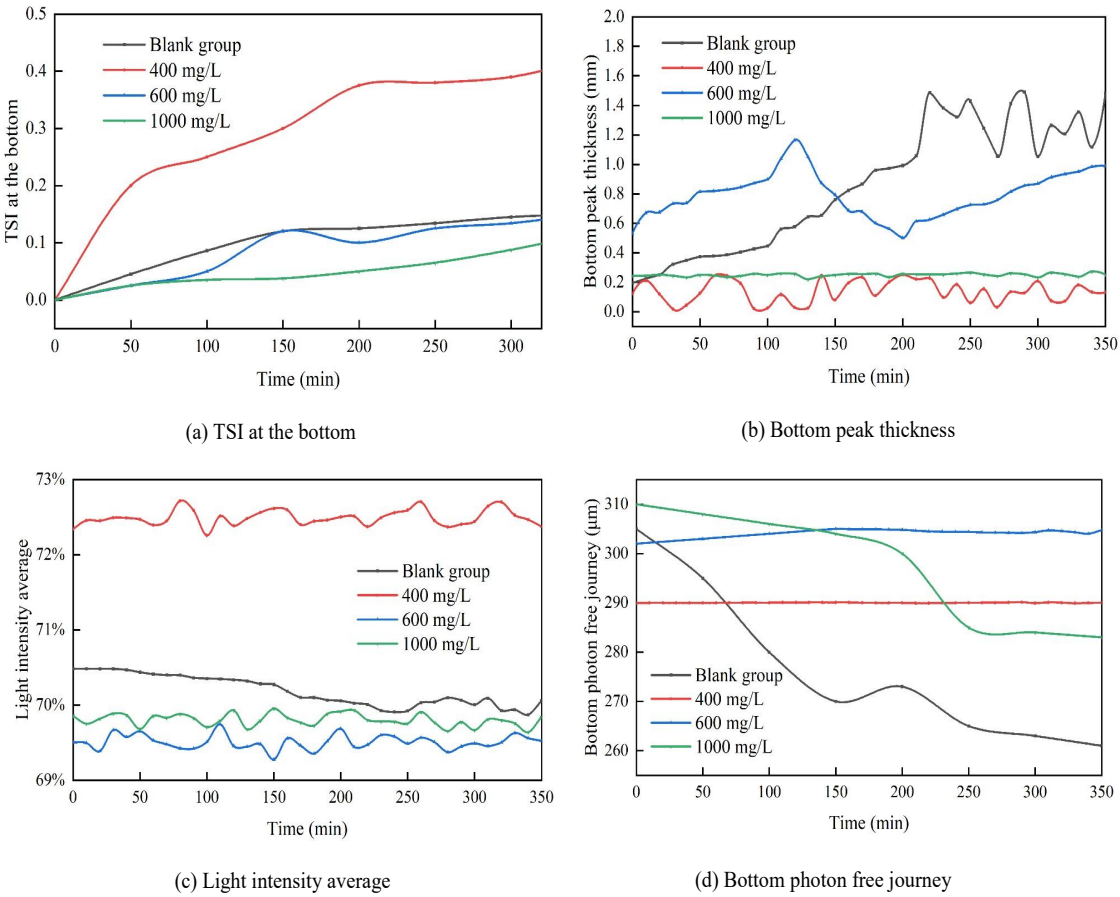

Fig. 4. Changes in indicators at the bottom under different TDS conditions

600 mg/L can effectively enhance the stability of nanoemulsified oil, but this enhancement effect gradually diminishes as the TDS increases. The changes in both peak thickness and light intensity showed good correspondence and correlation with TSI stability (R= 0.9173, $p<0.05$), confirming the reliability of the above results.

Both the TSI value variation and the peak thickness variation in the top unstable region are determined based on the backscattered light intensity (BS) variation, and the square of the backscattered light intensity is generally inversely proportional to the photon free range. Fig. 3(d) shows the characteristics of the photon free range variation in the top instability region. With increasing time, the photon free range of the blank group changed most drastically, while the 1000 mg/L sample was the second most drastic and the 400 mg/L and 600 mg/L showed the least change. This indicates that the kinetic indices of the 400 mg/L and 600 mg/L samples have less variation and better stability. The increasing trend of photon free range in the top unstable region in this experiment can be speculated that only the presence of droplet upwelling leading to the increase of upper concentration or particle size aggregation will make the backscattered light intensity increase with time.

Dynamics of stability parameters in the bottom instability zone

The variation of the backscattered light intensity in different regions of the sample shows that, in addition to the instability in the top instability region, the instability in the bottom instability region is also one of the factors that cause the overall stability of the sample to decrease. Fig. 4 shows the variation characteristics of TSI value, peak thickness, mean value of backscattered light intensity and photon free range in the bottom

unstable region of nanoemulsified oil under the influence of TDS. The results of TSI dynamics in the bottom unstable region show that the stability index of nanoemulsified oil increases with time, which is in the same direction as the stability change in the top unstable region, but its TSI value changes below 2.0, while the change value in the top unstable region is below 4.0. The thickness change of the peak thickness of the bottom instability zone is in a slight increase, but the thickness change of the top instability zone is below 4 mm, while the thickness change of the bottom instability zone is below 2 mm. It can be seen that although the kinetic index of the bottom instability zone also shows the instability of the sample, the variation of the bottom instability zone is smaller than that of the top instability zone, and the upward expansion ability of the bottom instability zone of nanoemulsified oil is weaker than the downward expansion ability of the top instability zone.

The TSI values and their variations in the bottom instability zone of nanoemulsified oils with TDS concentrations of 400 mg/L and 1000 mg/L were relatively small and the variations were about 33.3% and 66.7% of those of the blank group and 600 mg/L, respectively. The variation of TSI in the bottom instability zone of nanoemulsified oil with 400 mg/L TDS was less than 0.5 and stabilized during the test time, indicating that the stability of the bottom instability zone of nanoemulsified oil was enhanced at this TDS concentration. In contrast, the increase in TSI values and the slope of the tangent line were larger for the blank group and 600 mg/L, indicating that the stability of the unstable zone of nanoemulsified oil was poor under these two systems. Fig. 4(b) shows that the peak thickness of the bottom instability zone varies from large to small with time as follows: blank group > 600 mg/L > 1000 mg/L > 400 mg/L. The peak thickness of the nanoemulsified oil of 400 mg/L TDS hardly changed during the test time, while the peak thickness of the nanoemulsified oil of 600 mg/L TDS had a greater variation and slope than that of the 1000 mg/L TDS sample, which indicates that the effect of TDS on the bottom instability zone in stability effect is not monotonically decreasing with the concentration change. Fig. 3(c) shows a slight decrease in the backscattered light intensity in the bottom instability zone with time, indicating that the concentration of nanoemulsified oil in the bottom region should be decreasing and upwelling occurs. Among them, the decrease value of backscattered light intensity of 400, 600 and 1000 mg/L samples is within 0.5%, while the change of light intensity of blank group is above 1%. Fig. 5(d) shows the characteristics of the variation of photon free range in the bottom zone, and the degree of variation from large to small is consistent with the top unstable zone, indicating that the TDS of 400 mg/L has the strongest suppression effect on the droplet uplift in the bottom unstable zone and the best stability.

Potential factors of TDS affecting the stability of nanoemulsified oil

The kinetic variation of stability parameters at the top and bottom under the influence of TDS was characterized to show the stability changes in its unstable region, and it was found that the stability of nanoemulsified oil was enhanced at suitable TDS concentration. To further investigate the potential factors of nanoemulsified oil stability affected by TDS, the variation of two main factors (particle size and volume fraction) affecting the stability of nanoemulsified oil was analyzed. The increase of particle size of emulsified oil will lead to the increase of physical retention of emulsified oil and clogging of porous media, which may lead to groundwater bypass and thus treatment failure in severe cases. The volume fraction is introduced to investigate the change in the ratio of oil phase to water phase in different regions due to the migration of nanoemulsified oil droplets. Fig. 5(a) shows the particle size variation characteristics in the top unstable zone. The average particle size of the top instability zone gradually increases, which leads to an increase in backscattered light intensity, an increase in TSI value and a decrease in stability. The largest increase in particle size occurred in the blank group, and only a slight increase in particle size occurred in the nanoemulsified oil with 400 mg/L and 600 mg/L TDS, and the particle size of the emulsified oil increased by 3.4% as the TDS increased to 1000 mg/L.

Fig. 6 shows the variation characteristics of the volume fraction of the two unstable zones of the nanoemulsified oil. The volume fraction of the emulsified oil in the top zone gradually increased, and its change characteristics were similar to the stability results, and the blank group was most severely affected by the uplift, which increased by 34.8%. And the up-floating phenomenon at

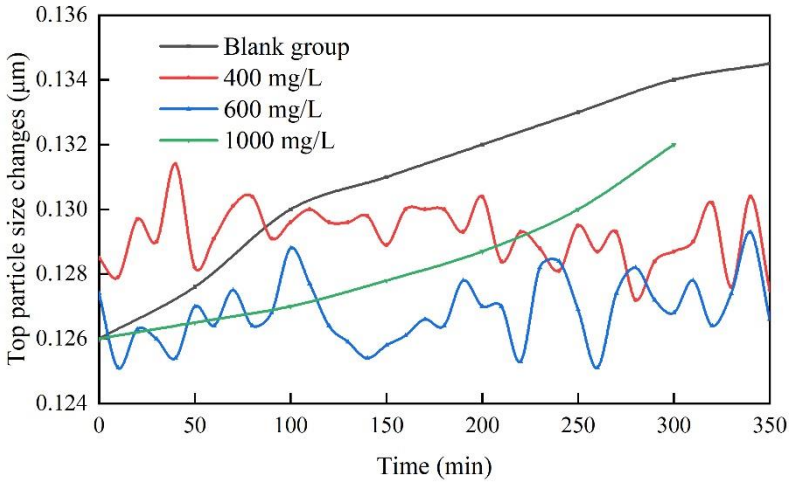

(a) Top particle size

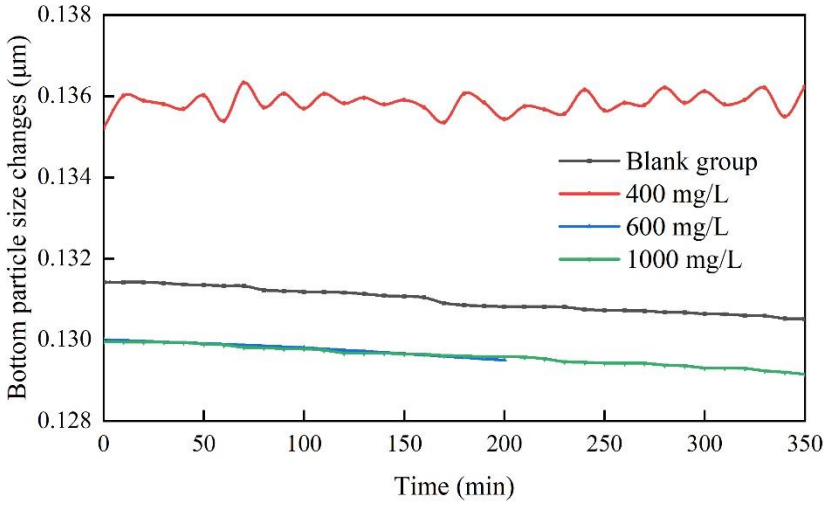

(b) Bottom particle size

Fig. 5. Particle size change in bottom unstable zone and top unstable zone

the top of the samples under the three TDSs was weakened by 88.5%, 93.8%% and 51.2% compared with the blank group. From the perspective of droplet aggregation, the uplift effect increased the distribution of nanoemulsified oil droplets in the upper part, and the effective collision-induced aggregation between droplets increased, leading to the instability of the unstable zone. As shown in Fig. 5(b), the particle size variation in the bottom instability zone is small, and only the particle size of the blank group decreases by 1.61 nm. The particle size variation of the emulsified oil at 400, 600 and 1000 mg/L TDS is not obvious, which indicates that the stability of the bottom zone is less affected by the particle size and its contribution to the reduction of the backscattered light intensity is less. The nanoemulsified oil in the bottom unstable zone also showed a decreasing trend in volume fraction because of the uplift, i.e., the uplift at the bottom of the samples under the three TDS was weakened by 78.7%, 76.8%, and 51.2% compared with the blank group. The

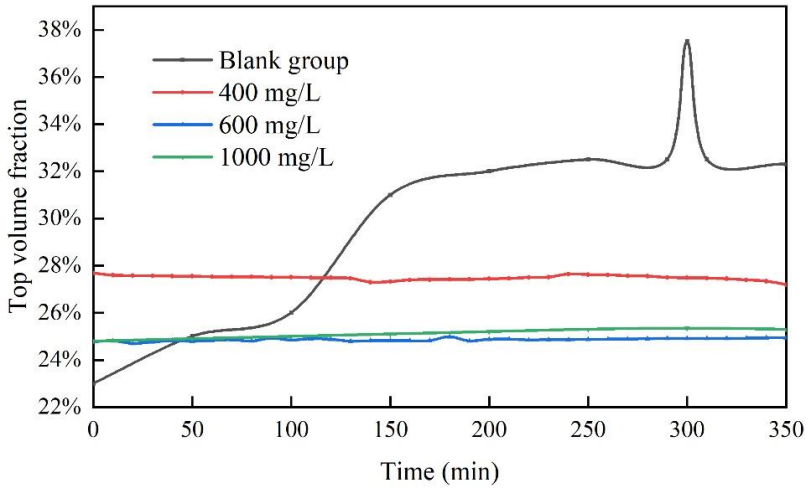

(a) Top volume fraction

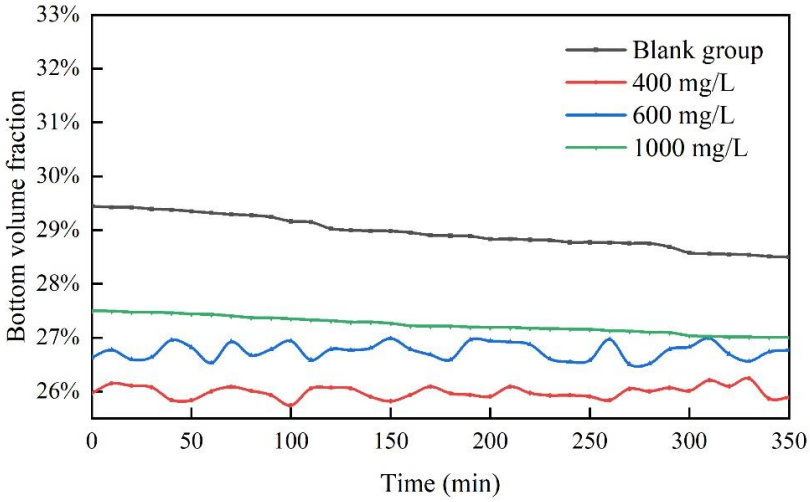

(b) Bottom volume fraction

Fig. 6. Volume fraction of nano-emulsified oil in the top and bottom zones

decrease in concentration due to the uplifting of bottom emulsified oil droplets may be the main reason for the decrease in backscattered light intensity in the bottom unstable region.

The variation of Brownian motion rate of nanoemulsified oil droplets under the influence of TDS is shown in Fig. 7. With the increase of TDS, the Brownian motion rate showed a trend of decreasing and then increasing. 400 mg/L and 600 mg/L samples showed weaker Brownian motion rate, i.e. weaker Brownian motion, and the probability of effective collision of droplets decreased, which increased the stability of nanoemulsified oil. In contrast, for the 1000 m/L sample, the Brownian motion rate increased, i.e., the Brownian motion was enhanced and the stability decreased. This may be related to the increase in viscosity of the aqueous phase of the emulsified oil and the increase in the gravitational force between the particles after the addition of salt. Compared to the blank group adding salt can make the viscosity of the foam system increase, but the increase of the viscosity of the system diminishes with the increase of the salt

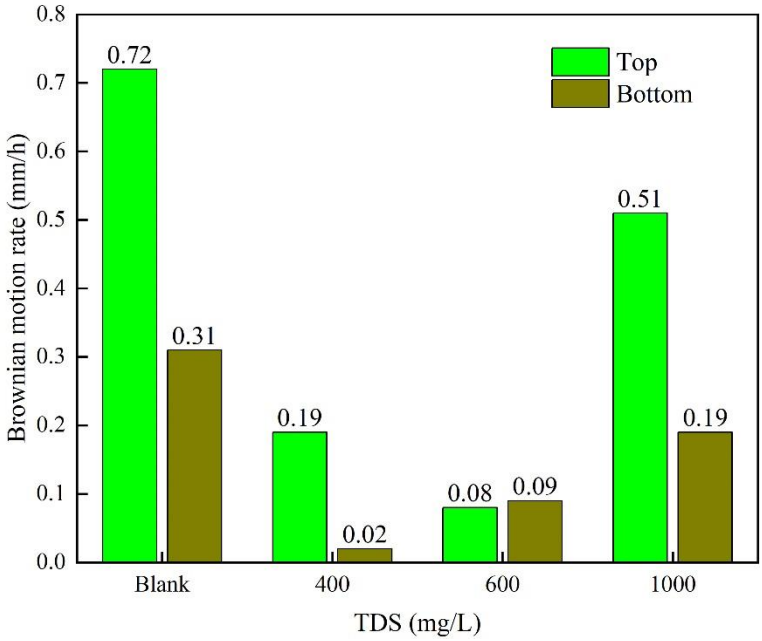

Fig. 7. Brownian motion rates in the top and bottom zones

concentration, and the different salt fractions make the viscosity increase to different degrees. This is because the addition of salt increases the viscosity of the nanoparticle system and increases the interparticle gravitational force. In this experiment, the viscosity of the aqueous phase of the emulsified oil increased with the increase of TDS, which weakened the Brownian motion of the particles, and the gravitational force between the droplets increased with the increase of TDS to 1000 mg/L. Under the effect of both viscosity and gravitational force, the stability of the samples was better than that of the blank group and lower than that of the low TDS samples.

Therefore, the instability of nanoemulsified oil is mainly influenced by the top instability zone and the bottom instability zone. The increase of instability in the top instability zone is due to the increase of volume fraction at the top due to the upward floating of the emulsified oil, which causes the increase of particle size due to the increase of effective collision of droplets. The instability in the bottom instability zone is smaller than that in the top zone, which is mainly influenced by the decrease of emulsified oil volume fraction due to the uplift. Combining the analysis of instability parameters and the results of Brownian motion rate, it can be seen that the Brownian motion rate is smaller for the TDS conditions of 400 mg/L and 600 mg/L, indicating that the Brownian motion is weakened, the chance of droplet collision is reduced, and the aggregation and uplifting will be weakened. The 400 mg/L sample was the most effective in suppressing the flotation phenomenon and aggregation with the best stability considering the change of stability in the top instability zone and bottom instability zone. This is similar to the results observed by other researchers in decane/water/Aerosol-OT and salt systems to reach the minimum salt concentration in the three-phase system occurs at 0.06 ~ 0. 09 mol/L and at 300 mmol/L salt for ionic surfactant emulsion systems with excellent stability. Therefore, the appropriate TDS conditions inhibit the uplift in the top unstable zone and bottom unstable zone, which leads to the increased stability of nanoemulsified oil.

CONCLUSION

In this paper, the effect of TDS on the stability of the prepared nanoemulsified oil was investigated by controlled experiments, and the following conclusions were drawn:

(1) TDS at concentrations of 0 ~ 1000 mg/L did have a positive effect on the stability of nanoemulsified oil, and this change in stability was mainly reflected in the ability to effectively

reduce the particle size and particle size variation, the TSI stability index, backscattered light intensity and photon free range variation showing a first decrease and then an increase.

(2) The instability of nanoemulsified oil was mainly manifested by the droplet uplifting phenomenon in the top instability zone and the aggregation and settling phenomenon in the bottom instability zone. The overall kinetic stability index showed that the order of stability under four TDS conditions was: 400 mg/L > 600 mg/L > 1000 mg/L > 0 mg/L. Under the appropriate TDS conditions, TDS positively influenced the stability of nanoemulsified oil and slowed down the instability of nanoemulsified oil.

(3) Suitable TDS conditions weakened the Brownian motion rate, which led to the weakening of the Brownian motion, resulting in the aggregation and weakening of the uplifting phenomenon, which was the main reason for improving the stability of nanoemulsified oil and alleviating the delamination of nanoemulsified oil. Compared with the blank group, the 400 mg/L nanoemulsified oil had the strongest alleviation effect on these two phenomena, with 87.5% and 79.4% alleviation of the uplift phenomenon in the top and bottom areas, respectively, and 87.2% alleviation of the aggregation phenomenon in the top area compared with the blank group.

CONFLICT OF INTEREST

The authors declare that there is no conflict of interests regarding the publication of this manuscript.

REFERENCES

1. Feng J, Esquena J, Rodriguez-Abreu C, Solans C. Key features of nano-emulsion formation by the phase inversion temperature method. Journal of Dispersion Science and Technology. 2020;42(7):1073-1081.
2. Xiong X. Research on tourism income index based on ordinary differential mathematical equation. Applied Mathematics and Nonlinear Sciences. 2022;7(1):653-660.
3. Borden RC, Lieberman MT. Passive Bioremediation of Perchlorate Using Emulsified Edible Oils. SERDP/ESTCP Environmental Remediation Technology: Springer New York; 2009. p. 155-175.
4. Linjie D, Jun D, Jing B, Zifang C. Migration and evolution of an in situ bioreactive zone formed with emulsified vegetable oil for the long-term remediation of nitrobenzene-contaminated groundwater. JHyd. 2021;593:125914.
5. Juárez Regalado FF, Esenarro D, Díaz Reátegui M, Frayssinet Delgado M. Model based on balanced scorecard applied to the strategic plan of a peruvian public entity. 3C Empresa Investigación y pensamiento crítico. 2021;10(4):127-147.
6. Wen C, Sheng H, Ren L, Dong Y, Dong J. Study on the removal of hexavalent chromium from contaminated groundwater using emulsified vegetable oil. Process Saf Environ Prot. 2017;109:599-608.
7. Mei D. What does students' experience of e-portfolios suggest. Applied Mathematics and Nonlinear Sciences. 2022;7(2):15-20.
8. Zhang J, Wu J, Chao J, Shi N, Li H, Hu Q, et al. Simultaneous removal of nitrate, copper and hexavalent chromium from water by aluminum-iron alloy particles. J Contam Hydrol. 2019;227:103541.
9. Maqache N, Swart AJ. Remotely measuring and controlling specific parameters of a PV module via an RF link. 3C Tecnología_Glosas de innovación aplicadas a la pyme. 2021;10(4):103-129.
10. Aswathanarayan JB, Vittal RR. Nanoemulsions and Their Potential Applications in Food Industry. Frontiers in Sustainable Food Systems. 2019;3.
11. Gong M. Study on tourism development income index calculation of finite element ordinary differential mathematical equation. Applied Mathematics and Nonlinear Sciences. 2022;0(0).
12. Sari TP, Mann B, Kumar R, Singh RRB, Sharma R, Bhardwaj M, et al. Preparation and characterization of nanoemulsion encapsulating curcumin. Food Hydrocolloids. 2015;43:540-546.
13. Frayssinet Delgado M, Esenarro D, Juárez Regalado FF, Díaz Reátegui M. Methodology based on the NIST cybersecurity framework as a proposal for cybersecurity management in government organizations. 3C TIC: Cuadernos de desarrollo aplicados a las TIC. 2021;10(2):123-141.
14. Muller KA, Esfahani SG, Chapra SC, Ramsburg CA. Transport and Retention of Concentrated Oil-in-Water Emulsions in Porous Media. Environmental Science & Technology. 2018;52(7):4256-4264.
15. Li T, Jin Y, Huang Y, Li B, Shen C. Observed Dependence of Colloid Detachment on the Concentration of Initially Attached Colloids and Collector Surface Heterogeneity in Porous Media. Environmental Science & Technology. 2017;51(5):2811-2820.
16. Zhang M, Lu X, Hoffman E, Kharabsheh R, Xiao Q. Radioactive source search problem and optimisation model based on meta-heuristic algorithm. Applied Mathematics and Nonlinear Sciences. 2022;7(2):601-630.
17. Pengon S, Chinatangkul N, Limmatvapirat C, Limmatvapirat S. The effect of surfactant on the physical properties of coconut oil nanoemulsions. Asian Journal of Pharmaceutical Sciences. 2018;13(5):409-414.
18. Tao F, Zhigao C. Smart Communities to Reduce Earthquake Damage: A Case Study in Xinheyuan, China. Applied Mathematics and Nonlinear Sciences. 2021;7(2):631-640.
19. Teo A, Goh KKT, Wen J, Oey I, Ko S, Kwak H-S, et al. Physicochemical properties of whey protein, lactoferrin and Tween 20 stabilised nanoemulsions: Effect of temperature, pH and salt. Food Chem. 2016;197:297-306.
20. Singh Yadav AK, Sora M. An optimized deep neural network-based financial statement fraud detection in text mining. 3C Empresa Investigación y pensamiento crítico. 2021;10(4):77-105.
21. Chang J, Lan W, Lan W. Higher education innovation and reform model based on hierarchical probit. Applied Mathematics and Nonlinear Sciences. 2021;7(1):175-182.

22. Dong J, Wen C, Liu D, Zhang W, Li J, Jiang H, et al. Study on degradation of nitrobenzene in groundwater using emulsified nano-zero-valent iron. Journal of Nanoparticle Research. 2015;17(1).
23. Meng S, Zhang X. Translog function in government development of low-carbon economy. Applied Mathematics and Nonlinear Sciences. 2021;7(1):223-238.
24. Nouri M, Baghaee-Ravari S, Emadzadeh B. Nano-emulsified savory and thyme formulation show limited efficacy to suppress Pectobacterium carotovorum subsp. carotovorum compared with pure oil. Industrial Crops and Products. 2021;161:113216.
25. Osama Horani M, Najeeb M, Saeed A. Model electric car with wireless charging using solar energy. 3C Tecnología_ Glosas de innovación aplicadas a la pyme. 2021;10(4):89-101.
26. Guan F, Cao J, Ren J, Song W. The teaching of sports science of track and field-based on nonlinear mathematical equations. Applied Mathematics and Nonlinear Sciences. 2021;7(1):191-198.
27. Ren G, Sun Z, Wang Z, Zheng X, Xu Z, Sun D. Nanoemulsion formation by the phase inversion temperature method using polyoxypropylene surfactants. Journal of Colloid and Interface Science. 2019;540:177-184.
28. Zhang H. Regression function model in risk management of bank resource allocation. Applied Mathematics and Nonlinear Sciences. 2021;7(1):661-668.
29. Ren G, Li B, Lu D, Di W, Ren L, Tian L, et al. Preparation of polyoxypropylene surfactant-based nanoemulsions using phase inversion composition method and their application in oil recovery. J Mol Liq. 2021;342:117469.
30. Rafati R, Oludara OK, Sharifi Haddad A, Hamidi H. Experimental investigation of emulsified oil dispersion on bulk foam stability. Colloids Surf Physicochem Eng Aspects. 2018;554:110-121.
31. Yang Y. Application of numerical method of functional differential equations in fair value of financial accounting. Applied Mathematics and Nonlinear Sciences. 2021;7(1):533-540.
32. Mei Z, Xu J, Sun D. O/W nano-emulsions with tunable PIT induced by inorganic salts. Colloids Surf Physicochem Eng Aspects. 2011;375(1-3):102-108.
33. Dewani A, Memon MA, Bhatti S. Development of computational linguistic resources for automated detection of textual cyberbullying threats in Roman Urdu language. 3C TIC: Cuadernos de desarrollo aplicados a las TIC. 2021;10(2):101-121.
34. Kawabe Y, Komai T. A Case Study of Natural Attenuation of Chlorinated Solvents Under Unstable Groundwater Conditions in Takahata, Japan. Bulletin of Environmental Contamination and Toxicology. 2019;102(2):280-286.
35. Liu Y. Analysis and Prediction of College Students' Mental Health Based on K-means Clustering Algorithm. Applied Mathematics and Nonlinear Sciences. 2021;7(1):501-512.
36. Qian C, Decker EA, Xiao H, McClements DJ. Physical and chemical stability of β-carotene-enriched nanoemulsions: Influence of pH, ionic strength, temperature, and emulsifier type. Food Chem. 2012;132(3):1221-1229.
37. Medina Rodríguez R, Breña Oré JL, Esenarro Vargas D. Efficient and sustainable improvement of a system of production and commercialization of Essential Molle Oil (Schinus Molle). 3C Empresa Investigación y pensamiento crítico. 2021;10(4):43-75.
38. Haugen KS, Semmens MJ, Novak PJ. A novel in situ technology for the treatment of nitrate contaminated groundwater. Water Res. 2002;36(14):3497-3506.
39. Julca Coscol ÁB, Tapia Prado CD, Hilario Falcón FM, Corpus Giraldo CM. Qualitative benchmarking study of software for switch performance evaluation. 3C Tecnología_Glosas de innovación aplicadas a la pyme. 2021;10(4):35-49.
40. He B, He J, Zou H, Lao T, Bi E. Pore-scale identification of residual morphology and genetic mechanisms of nano emulsified vegetable oil in porous media using 3D X-ray microtomography. Science of The Total Environment. 2021;763:143015.
41. Li J. Evolutionary game research on the psychological choice of online shopping of fresh agricultural products based on dynamic simulation model. Applied Mathematics and Nonlinear Sciences. 2021;7(1):703-710.
42. Beheshti E, Riahi S, Riazi M. Impacts of oil components on the stability of aqueous bulk CO2 foams: An experimental study. Colloids Surf Physicochem Eng Aspects. 2022;648:129328.
43. Hao L. Differential equation model of financial market stability based on big data. Applied Mathematics and Nonlinear Sciences. 2021;7(1):711-718.
44. Shen S. Multi-attribute decision-making methods based on normal random variables in supply chain risk management. Applied Mathematics and Nonlinear Sciences. 2021;7(1):719-728.
45. Li G, Yao D, Wang Y. Data Reconstruction for a Disturbed Soil-Column Experiment Using an Optimal Perturbation Regularization Algorithm. Journal of Applied Mathematics. 2012;2012:1-16.
46. Yang Y. Linear fractional differential equations in bank resource allocation and financial risk management model. Applied Mathematics and Nonlinear Sciences. 2021;7(1):729-738.
47. He B-n, He J-t, Wang F, Lian Y-q, Zhao Y-k. Migration, clogging, and carbon source release of nano emulsified vegetable oil in porous media, evaluated by column experiments. Bioremediation Journal. 2018;22(1-2):53-62.
48. Kaseng F, Lezama P, Inquilla R, Rodriguez C. Evolution and advance usage of Internet in Peru. 3C TIC: Cuadernos de desarrollo aplicados a las TIC. 2020;9(4):113-127.